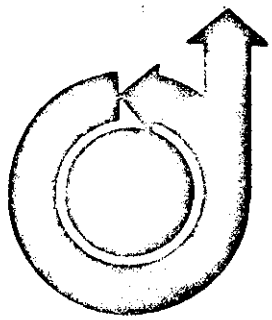

AIAA Paper No. 74-149

(3)

BLAST INITIATION AND PROPAGATION OF CYLINDRICAL DETONATION IN MAPP-AIR MIXTURES

by
R. S. FRY and J. A. NICHOLLS
University of Michigan
Ann Arbor, Michigan

AIAA PAPER 74-149

AIAA 12th Aerospace Sciences Meeting

WASHINGTON, D.C. / JANUARY 30-FEBRUARY 1, 1974

(9)

BLAST INITIATION AND PROPAGATION OF CYLINDRICAL DETONATIONS IN MAPP-AIR MIXTURES*

R.S. Fry** and J. A. Nicholls†
University of Michigan
Ann Arbor, Michigan

Abstract

An experimental investigation of the initiation, transition and quasi-steady propagation of blast initiated cylindrical detonations in Methyl Acetylene, Propane, Prodadiene (MAPP)-air mixtures is described. A sectored shock tube was employed which was originally designed to allow study of cylindrical shock, homogeneous and heterogeneous detonation waves. Experimental data served to suggest the existence of three wave propagation regimes: subcritical energy regime, where decoupling of shock and reaction zone results in a reacting blast wave type decay; the critical energy regime, where decoupling occurs but is followed by the reestablishment of a sub-Chapman-Jouguet condition, with an asymptotic strengthening to the CJ state; and supercritical energy regime, where the initially overdriven detonation decays asymptotically to its CJ state. Critical ignition energy limits, prescribing the location of the second regime, were established as a function of blast wave energy for a full volumetric range of MAPP-air mixtures. Comparisons made with work of other researchers reveal these limits do not suffer from scale effects. Throughout all mixtures examined wave strength displayed a strong dependence on initial blast wave energy, while still comparing favorably with theory. Similarly, critical ignition distances compared satisfactorily with theoretical critical radii for all mixtures, when non-dimensionalized by blast wave explosion length.

I. Introduction

In recent years much concern has been generated regarding the frequent occurrence of accidental ignition and subsequent explosion of large unconfined vapor clouds. Explosions are commonly thought of as occurring in a confined environment such as in vessels, pipes, sewers, homes and the like. On the other hand it has become increasingly evident that unconfined explosions may be generated in the atmosphere. As pointed out by Strehlow[1], the explosion of unconfined vapor clouds by the dispersion of flammable liquid or vapor spills is becoming a serious problem, mainly because of the increased size of these spills. Further, there has been interest in deliberate fuel-air explosions wherein a liquid or gaseous fuel is dispersed throughout a volume of the atmosphere and detonated. To date quantitative experimental studies of unconfined explosions are essentially non-existent and therefore current practice of dange assessment and/or risk evaluation is based on the estimate of a TNT equivalent from the damage patterns assuming a point source blast wave energy release. It is known, however, that unless the cloud detonates, the explosion itself and the blast wave it produces are far from ideal and cannot be approximated adequately by classical self-similar solutions. Theory substantiated by experiment has succeeded in classifying the attendant wave phenomena into energy dependent regimes. In any case, the exact energy release rate is of fundamental importance and is very dependent on initial conditions, such as spill geometry, fuel distribution, turbulence and buoyancy effects, and the type and energy of the ignition source.

Due to the complex nature of unconfined fuel-air explosions a detailed analytic solution is not completely possible, and a satisfactory model must rely additionally upon experiment.

The reviews of Lee[2], Chernyi et al[3], and Korobeinikov[4] summarize recent work on blast propagation through combustible mixtures. In discussing the propagation of blast waves through combustible mixtures[5] it is useful to define a critical blast wave radius r_* such that the energy of combustion contained within r_* is equal to the blast wave energy E_o. If Q is the combustion energy per unit mass of fuel oxidizer mixture, then

$$r_* = (\nu E_o / \sigma_\nu Q \rho_1)^{1/\nu} \qquad (1)$$

where $\nu = 1, 2, 3$ and $\sigma_\nu = 2,\ 2\pi,\ 4\pi$ for planar, cylindrical, and spherical waves. When the blast radius $r_s \ll r_*$, the blast energy E_o is dominant and asymptotic analysis[6] shows that the flow then can be described by the self similar strong

*This work was supported by the Air Force Armament Laboratory, Eglin Air Force Base, under Contract F08635-71-C-0083.
**Graduate Student, Aerospace Engineering.
†Professor, Aerospace Engineering.

blast wave solution of Sedov[7], and Taylor[8]. When $r_s >> r_*$ combustion dominates and the blast wave decays to a constant velocity Chapman-Jouguet (C-J) detonation, provided combustion is instantaneous at the shock front. The flow behind the C-J wave also is self similar[7]. In the transitional region $r_s \sim O(r_*)$ the flow is no longer self similar and various numerical, perturbation, and approximation techniques used to deal with this region are described by Lee[2] and Korobeinikov[5].

The theory[5,6] shows that transition to a C-J detonation always occurs when the combustion energy is released instantaneously, i.e. when the reaction zone thickness, Δ, behind the shock front is negligibly small. With finite Δ, the one dimensional analysis of Korobeinikov et al.[9] shows that the flame zone separates from the leading shock, thus precluding the formation of a steady C-J detonation. This is in conflict with the fact that all detonations have a finite reaction zone thickness and blast initiated detonations have been observed. In view of this difficulty, Bach et al.[10] have introduced a phenomenological theory of initiation. They find that with a finite reaction zone thickness Δ, transition to a C-J detonation will only occur when the blast energy E_o exceeds a certain critical initiation value in accord with experimental observation. In terms of a characteristic explosion length, r_o, defined by

$$r_o = \left(\frac{E_o}{k_\nu \rho_1 a_1^2}\right)^{\frac{1}{\nu}} = \left(\frac{E_o}{k_\nu \gamma_1 p_1}\right)^{\frac{1}{\nu}} \qquad (2)$$

blast initiation of a C-J detonation occurs only when the ratio (Δ/r_o) is less than a certain critical value. Here $k_\nu = 1, 2\pi, 4\pi$, for $\nu = 1, 2, 3$, and a_1 is the speed of sound in the unburned fuel oxidizer mixture.

The model recovers the two limiting cases of a supercritical energy regime (i.e., a monotonic decay to a C-J wave) for very large initiation energy and the subcritical energy regime (i.e., the blast asymptotically approaches an acoustic wave) for very low source energy. In between the two limits the blast initially decays to sub-Chapman-Jouguet velocity and then slowly accelerates, eventually approaching the C-J condition. The model predicts that the minimum velocities reached depend on the magnitude of the ignition energy. This solution suggests that unless the initiation energy is extremely large, a decay below the C-J condition always occurs and the eventual approach is rather slow. An interesting feature of the theory is the occurrence of stable sub-C-J waves when Δ/r_o is near the critical initiation value. While some experimental verification of this theory exists, in the main, it has yet to receive wide acceptance.

The theoretical developments described above require considerable computation, particularly in the transitional region, $r_s \sim O(r_*)$. The theory of initiation is, in any case, only in a preliminary form. There are, however, a number of practical problems where the main features of blast propagation through explosive mixtures are desired with minimum computational effort. The results of Bach et al.[10], Korobeinikov[5] and Chernyi et al.[3] show that the transition from blast to C-J wave behavior, if it takes place, occurs when $r_s \sim r_*$, for both discontinuous and finite thickness detonation fronts. Korobeinikov[5] shows that the distributions of velocity, pressure, and density correspond to those behind a strong blast wave when $r_s/r_* << 1$, and to those behind a C-J detonation when $r_s/r_* >> 1$. In the zeroth order solution it is assumed that the blast wave property variations are valid for $r_s < r_*$ while the C-J property distributions are used for $r_s > r_*$. Of course this simplification precludes description of the transitional flow and hence cannot predict initiation energies.

The research described here is part of an ongoing theoretical and experimental study[11,12,13] of cylindrical shock, homogeneous and heterogeneous detonation waves aimed at gaining a better understanding of the complex problem of the unconfined explosion of fuel-oxidizer mixtures. The immediate scope toward which this paper is directed involves an experimental investigation of the overall wave propagation characteristics in strong blast wave initiated cylindrical gaseous detonations. In particular, the initiation, transition and quasi-steady propagation of cylindrical detonations in Methyl Acetylene, Propane, Propadiene (MAPP)-air mixtures has been studied.

II. Experiments

As indicated in the Introduction, many questions remain in connection with the propagation of blast waves in combustible mixtures. Accordingly, it was of interest to conduct controlled experiments in order to overcome the theoretical limitations. To this end it became desirable to select an experiment that; (i) permits detailed measurements on a non-planar system, (ii) lends itself to a theoretical description, and (iii) is small and safe enough to allow experiments inside a laboratory.

To accommodate these features an idealized cylindrical cloud was modeled. Due to the axial symmetry of the problem and in order to minimize the size of the explosion, the test chamber configuration chosen was a pie shaped sector.

Now the walls of a detonation chamber will affect the detonation process by heat and momentum losses throughout the reaction zone. Such losses are in general greater for heterogeneous detonation waves due to its extended reaction zone being a function of fuel drop size. Since the chamber must also accommodate this type of testing, this entered the design considerations. Further, spatial limitations associated with the method of producing drops had to be considered. In general very few chamber design limitations were established by the homogeneous wave phase of the research. These and other factors, more nearly associated with the heterogeneous research phase, were taken into account[11], in arriving at the final design shown schematically in Fig. 1. Fundamental alterations to the fuel system were made to accommodate gaseous fuels, as shown in Fig. 2. The openings in the liquid drop injection system, as well as other leakage spots, are sealed prior to conducting any tests. Blast wave initiation is achieved by the firing of a blasting cap and a controlled amount of Detasheet at the apex of the sector. Thus cylindrical shock waves and, under the right conditions, heterogeneous detonation waves are generated. Wave arrival times are determined by a number of pressure switches and pressure distributions by 3 transducers. The detonation chamber, without the breech-like explosive charge holder, is 28 3/4 inches along the centerline. The included angle between the top and bottom bars is 20°. The inside dimensions of the chamber are 2.05 inches wide, 1 inch high at the initiator end, and 11 inches high at the open end.

Considerable emphasis was initially placed on the attainment of good blast wave data. The reasons for this are basically three-fold. First, it was an expedient way to debug much of the apparatus and instrumentation and to gain experience and confidence in the operation. Second, it was deemed important to assess the degree to which cylindrical blast waves were being generated. Third, good documentation and understanding of the blast wave data provided an experimental technique for the determination of initiation requirements for the two-phase detonation. To fulfill the second requirement, it was of interest to interpret the experimental blast results in light of cylindrical theory. In order to do this, it was necessary to determine both the theoretical geometric origin and the time origin of the modeled line-source explosion. The blast center $r = 0$ was assumed to be at the hypothetical apex of the chamber. Then it was necessary to determine the effective time it would take a blast wave to travel from the origin to the oscilloscope trigger station. Blast wave data was then adjusted by this effective time, referencing it to the origin of an ideal modeled line source. The data was then regressed to the generalized mathematical form

$$t = a\, r^n \qquad (3)$$

to examine how closely it followed the radius-time behavior of strong cylindrical blast wave theory, where

$$t = b\, r^2 \qquad (4)$$

The regression revealed, that for all blast energies examined, $1.5 \leq n \leq 1.9$ nominally, where n tended to increase slightly with increasing energy. This is in agreement with work by Cole[14], who determined n for a wide range of shock strengths and several ambient atmospheres. A plot of radius-time data non-dimensionalized by blast explosion length for several source energies is given in Fig. 3. Plotted with this data is classical cylindrical theory for instantaneous energy release. The fundamental features of this figure are the asymptotic manner in which experiment approaches theory with increasing r/r_o; better general agreement as energy increases; and overall good agreement between experiment and theory. Any lack of agreement between experiment and the classical self-similar blast wave theory with instantaneous energy release can be traced to inherent non-idealities which exist both in the experimental apparatus and in the physics of the wave process. The existence of a physically limiting chamber causes energy losses to the walls and leakage through parts in the detonator breech. The initiation energy release is not instantaneous as assumed, but actually calculated to be of the order of 10 μsec. The blast energy is not released uniformly along a line source. Finally, energy losses may be attributed to dissociation and ionization of the expanding gas behind the leading shock which lead to wave attenuation. For the reasons outlined and from the analysis of the blast wave data it was found that the energy release experienced in the sectored chamber was less than that predicted from a known quantity of Detasheet used with the detonator. An estimate of energy efficiencies were computed by comparing the experimental data regressed following Eq. 4 and the radius-time variation from strong cylindrical blast wave theory given in Eq. 5

$$t = (E_o/\rho_1)^{-1/2}\, r^2 \qquad (5)$$

An energy efficiency is now defined as

$$\eta_e = E_{o_{reg}} / E_{o_{calc}} \qquad (6)$$

Here $E_{o_{reg}}$ follows directly from a mathematical regression to experimental data; while $E_{o_{calc}}$ is

derived from knowledge of the detonator-Detasheet combination. Energy efficiencies have been determined for a range of energies for which experimental blast wave data was taken. Figure 4 gives the results of this computation. The curve displayed is a second order polynomial regression to all the data, and was used to describe the energy efficiency in subsequent computations.

It is concluded from this discussion of blast results that the experiments approximate the desired cylindrical blast wave behavior fairly well.

With the facility calibrated using the blast wave experiments, gas phase detonation experiments were conducted. The initial pressure and temperature correspond to room conditions and eight different equivalence ratios were tested. A systematic variation of initiation energy was tested for each equivalence ratio so that threshold energy conditions for the establishment of detonation could be determined. Figure 5 is a typical radius-time plot of experimental detonation data at a given energy, demonstrating the current technique for obtaining experimental detonation wave propagation velocity and critical transition distance. Such data is obtained for several energies at each mixture ratio, and examined to reveal a threshold energy below which an apparent steady detonation is not obtained.

A gas chromatographic analysis was made upon samples of the pure gas as well as on the eight MAPP-air mixtures. The significant properties of the MAPP gas used are shown in Table I.

Table 1 MAPP Gas Properties

Molecular weight	41.0
Density (slugs/ft^3)	0.1126
Stoichiometric equivalence ratio (O_2 basis)	0.302
Composition	
Methyl Acetylene	51.0%
Propane	26.0%
Propadiene	23.0%

Figures 6 and 7 display in transparent fashion the fundamental wave behavior of MAPP-air detonations, for 9.7% and 4.3% MAPP by volume respectively, as a function of chamber radial distance and initiation energy. They are intended to be representative of all the essential observed wave phenomena. Orientation of this Mach number-radius data relative to Bach et al's[10] phenomenological model will serve to clarify further discussions. If non-dimensionalized, the r/r_o would nominally fall between the limits 0.4 to 0.7. This is approximately the predicted location of the energy-dependent minimum velocities. This is important in as much as experimental detonation Mach numbers were all determined to be monotonically increasing function of initiation energy. Physically then it is apparent that a very small velocity change in the region $0.4 \leq r/r_o \leq 0.7$ is being measured and consequently being referred to as a quasi-steady sub-Chapman-Jouguet state. For sufficiently low initiation energy the wave clearly proceeds to follow a continually decaying reacting blast wave pattern. An additional interesting feature of Fig. 6 for 9.7% MAPP is that at a definitely sub-threshold energy level, a detonation wave behavior is followed, yet at a clearly sub-M_{CJ} level. This serves to establish experimentally the existence of a region of unstable wave propagation phenomena. It further substantiates another of the concepts of the phenomenological theory. Figure 7 for 4.3% MAPP again reveals the monotonic dependency of experimental Mach number, M_{Exp}, upon initiation energy. Of course both Fig. 6 and Fig. 7 easily show the existence of critical ignition distances, about which more will be said later. Again a threshold energy level is visible where a large fall in M_{Exp} occurs and where the curves begin to decay rapidly. A fundamental difference between Fig. 6 and Fig. 7 is that in the former, $M_{Exp} < M_{CJ}$; while in the latter, $M_{Exp} \leq M_{CJ} \leq M_{Exp}$. The reason for this is that for 9.7% MAPP the highest initiation energy run conducted and the determined threshold energy were both of the same order of magnitude. This was due primarily to energy limitations of the chamber breech and safety considerations. For the 4.3% MAPP mixture, however, the highest initiation energy used was near approaching an order of magnitude higher than the final determined threshold energy. While this point appeared universal throughout most of the data, some cases satisfied it in a stronger fashion than others. Figure 8 is a plot of mean experimental detonation Mach number compared with theoretical M_{CJ} plotted against MAPP volumetric concentration. For the concentrations of 3.3% through 6.8%, which experienced the supercritical propagation regime, $3. \leq E_{Max}/E_{crit} \leq 9.$ Anamalous behavior is revealed at the very lean mixture ratio of 2.9%, so the strange experimental behavior should not be all too unexpected. Additionally, significant discrepancies have, however, been noted for weak mixtures near the limits of detonability and characterized by incomplete chemical reactions. Since 9.7% MAPP by volume is also considered a weak mixture relative to say a mixture of 50% Acetylene, it too probably suffered from these effects.

An interesting result is revealed if the ratio $E_{crit}/E_{M_{CJ}}$ is computed for each MAPP-air concentration. Define E_{crit} here as the experimentally determined threshold energy and $E_{M_{CJ}}$ as the experimental energy at which theoretical M_{CJ} is achieved. It is found that this ratio

is minimized for stoichiometric mixtures and is much less than 1.0. That is, the energy step from E_{crit} to $E_{M_{CJ}}$ is maximized for stoichiometric mixtures.

Critical ignition distances obtained from detonation radius-time data can be non-dimensionalized using explosion length, r_o. It is known that the ratio of critical radius, r_*, to explosion length can be given[13] as

$$\frac{r_*}{r_o} = \frac{2}{M_D}(\gamma_2^2 - 1)^{1/2} \qquad (7)$$

for cylindrical geometry. It is hence a constant for a given fuel mixture ratio. Thus it was in order to non-dimensionalize experimental r_* data by r_o and average all r_*/r_o ratios for a given mixture ratio. The results of this calculation are compared with theory in Fig. 9. Satisfactory agreement is seen with a nominal error of 10%, with much closer agreement in most cases.

The threshold energies determined as a function of mixture ratio are shown in Fig. 10. The limits of detonability found for the MAPP gas used were from 2.9 percent to 10.5 percent by volume. The rich limit is an extrapolation of data taken up to a MAPP concentration of 9.7 percent. It is of interest to examine these detonation limits in light of other recent experimental results. Table II represents a comparison of detonation limits on a percent volume basis between four separate experimental studies. By using the Crawshaw-Jones Apparatus[15], it was found that detonation limits of MAPP-air mixtures widened with increasing initiator energy. Yet the bag tests of Benedick et al[16] and Collins[17] did not confirm this functional dependency. Similarly, the present study, using initiator energies two orders of magnitude smaller than the latter two studies, tends to cast doubt upon such a dependency. The good agreement between our data and the bag tests suggests that theCrawshaw-Jones apparatus is not reliable for high energy levels.

A further comparison was performed to examine the critical threshold energy limits of the present study relative to those of recent AFATL bag tests by P. Collins[17]. Figure 11 is a plot of nondimensional critical threshold energy as a function of MAPP concentration by weight for the two mentioned studies. The nondimensional energy, $\bar{E}$, was arrived at by dividing all energies for a given study by an energy selected from this data as the standard. The standard for each study was the value of critical energy corresponding to 11.7 percent MAPP by weight. This standard is not absolute, but rather it was conveniently chosen to demonstrate relative trends in critical energy since data was obtained in both studies at this MAPP concentration. The comparison reveals the present study produced data suggesting a slightly broader and slightly shallower characteristic threshold curve. The broader detonability limits in the present study are supported by the fact that the MAPP gas used had a higher percent of methyl acetylene present as compared to the MAPP used in the bag tests. The composition of the MAPP used in the bag tests is reported to have approximately the composition 37 percent methyl acetylene, 25 percent prodadiene, 20 percent propane, 9 percent C_4-carbon compounds (mostly n-butane) by volume.

III. Conclusions

The sectored shock tube is proving to be a useful tool in the study of the propagation of blast waves in gaseous and heterogeneous combustible mixtures. Experimental data has served to substantiate the existence of multi-regimes wave propagation phenomena. Reliable cylindrical blast wave critical radius, blast wave to detonation transition, threshold energy, detonation and detonation limit data are being obtained.

Table II Detonation Limits of MAPP-Air Mixtures by Volume

Method	Initiator	Lower Limit	Upper Limit
Crawshaw-Jones Apparatus	1 gram, PETN	4.1	7.8
Crawshaw-Jones Apparatus	10 grams, PETN	2.4	13.7
Crawshaw-Jones Apparatus	100 grams, PETN	-	$\geq$ 30
Bag Test	800 grams, C-4 (672 grams, PETN equivalent)	2.9	10.2
Bag Test	386 grams, PETN	2.9	9.1
Sectored Chamber	2 grams Detasheet 'C' (1.57 grams, PETN equivalent)	2.9	10.5[a]

[a]Extrapolated from test results taken up to 9.7 percent by volume.

References

1. Strehlow, R.A., "Unconfined Vapor Cloud Explosions—An Overview," Fourteenth Symposium (International) on Combustion, The Combustion Institute, Pittsburgh, Pennsylvania (1973) pp. 1189-1198.

2. Lee, J.H., "Gasdynamics of Detonations," Astronautica Acta, 17, (1972) pp. 455-466.

3. Chernyi, G.G., Korobeinikov, V.P., Levin, V.A., and Medvedev, S.A., "One-Dimensional Unsteady Motion of Combustible Gas Mixtures Associated with Detonation Waves," Astronautica Acta, 15, (1970), pp. 259-266.

4. Korobeinikov, V.P., "Gas Dynamics of Explosions," Annual Review of Fluid Mechanics, 3, (1971) pp. 317-346.

5. Korobeinikov, V.P., "The Propagation of Point Explosions in a Detonating Gas," Astronautica Acta, 14, (1969), pp. 411-419.

6. Levin, V.A. and Chernyi, G.G., "Asymptotic Laws of Behavior of Detonation Waves," P.M.M., 31, (1967), pp 393-405.

7. Sedov, L.I., Similarity and Dimensional Methods in Mechanics, Academic Press, New York, (1959).

8. Taylor, G.I., "The Dynamics of the Combustion Products Behind Plane and Spherical Detonation Fronts in Explosives," Proc. R. Soc., A200, (1950), pp. 235-247.

9. Korobeinikov, V.P., Levin, V.A., Markov, V.V., and Chernyi, G.G., "Propagation of Blast Waves in a Combustible Gas," Astronautica Acta, 17, (1972), pp. 529-537.

10. Bach, G.G., Knystautas, R., and Lee, J.H., "Initiation Criteria for Diverging Gaseous Detonations," 13th Symp. (Int.) on Combustion, The Combustion Institute, Pittsburgh, Pa., (1971), pp. 1097-1110.

11. Nicholls, J.A., Fry, R.S., Glass, D.R., Sichel, M., Vander Schaff, J., and Sternstein, A.J., "Fundamental Aspects of Unconfined Explosions," Technical Report, AFATL-TR-72-49, March, (1972).

12. Nicholls, J.A., Sichel, M., Fry, R.S., Hu, C., Glass, D.R., DeSaro, R., and Kearney, K., "Fundamental Aspects of Unconfined Explosions," Technical Report, AFATL-TR-73-125, March (1973).

13. Nicholls, J.A., Sichel, M., and Fry, R.S., "Theoretical and Experimental Study of Cylindrical Shock and Heterogeneous Detonation Waves," Fourth International Colloquium on Gasdynamics of Explosions and Reactive Systems, July (1973) (in press).

14. Cole, A.L., "A Study of Cylindrical Shock Waves in a Sectored Shock Tube," Ph.D. Thesis (1961).

15. Burgess, D.C., Murphy, J.N., Hanna, N.E., and Dolah, R.W., "Large-Scale Studies of Gas Detonations," Bureau of Mines Report of Investigations 7196 (1968).

16. Benedick, W.B., Kennedy, J.D., and Morosin, B., "Detonation Limits of Unconfined Hydrocarbon-Air Mixtures," Combustion and Flame, 15, (1970) p. 83.

17. Collins, D.M., "Critical Energy Threshold for Detonation Initiation in MAPP-Air Mixtures," AFATL-TR-72-192, (1972).

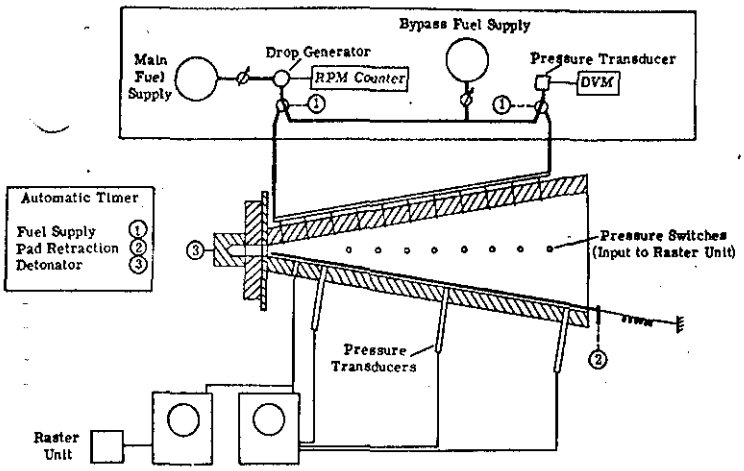

Figure 1. System Schematic.

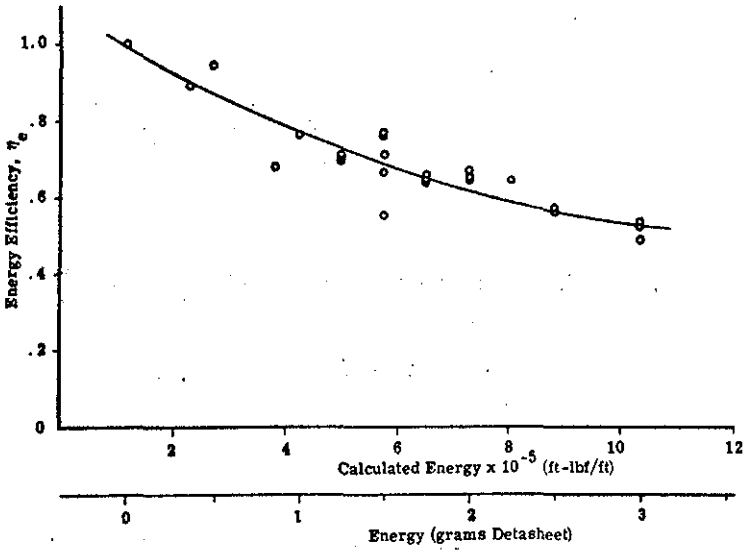

Figure 4. Sectored Chamber Engrgy Efficiency as a Function of E_o.

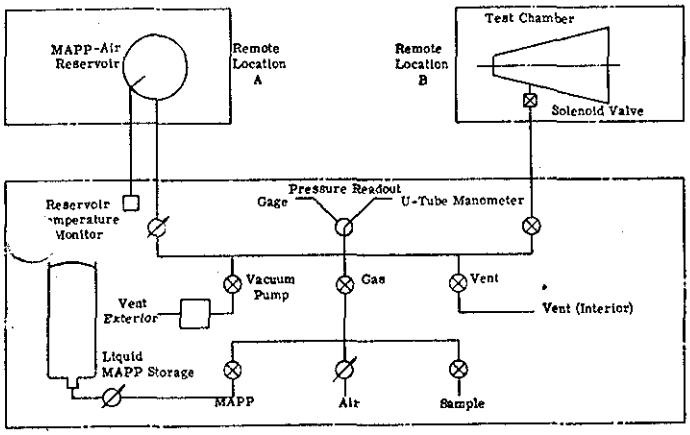

Figure 2. Schematic of Gas Detonation Apparatus

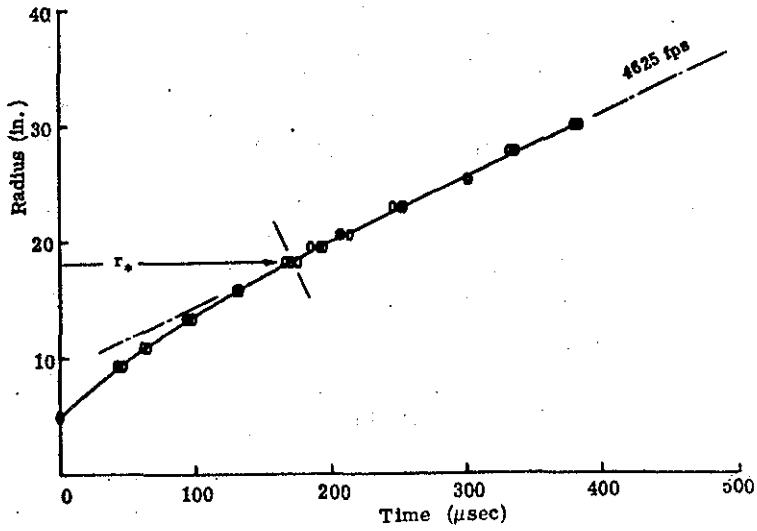

Figure 5. Data Reduction Technique.

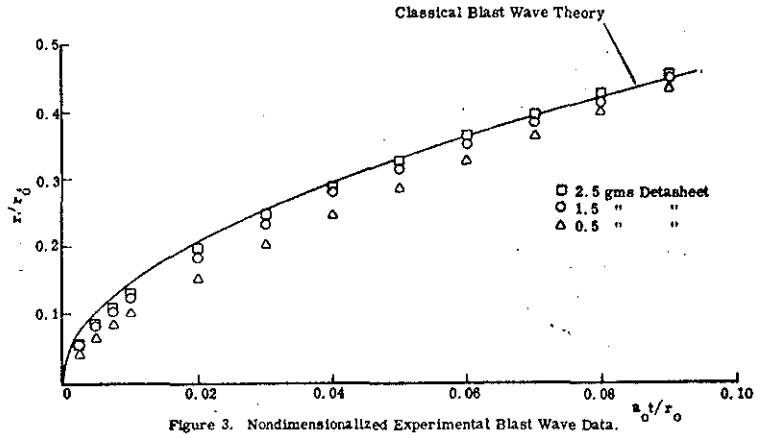

Figure 3. Nondimensionalized Experimental Blast Wave Data.

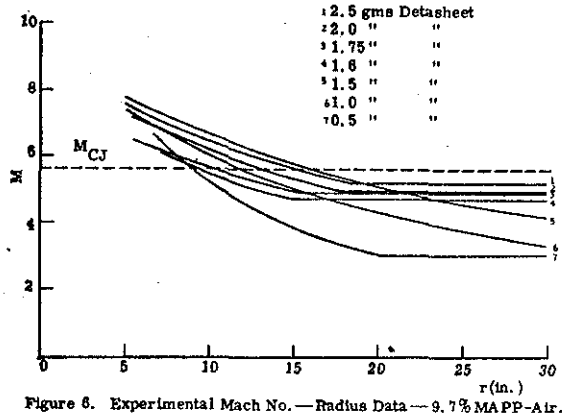

Figure 6. Experimental Mach No. — Radius Data — 9.7% MAPP-Air.

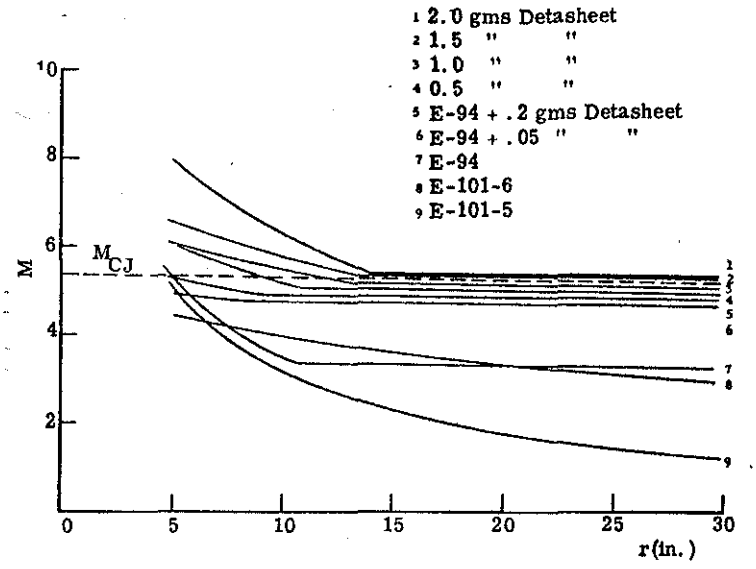

Figure 7. Experimental Mach No. — Radius Data — 4.3% MAPP-Air.

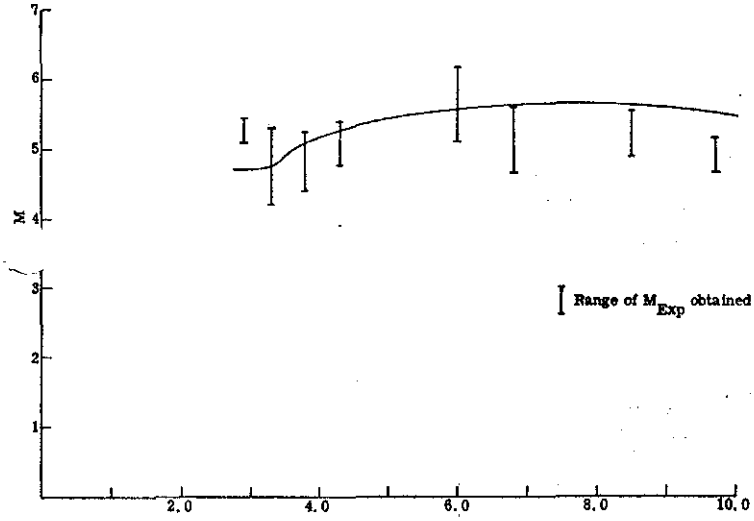

Figure 8. M_{Exp} and M_{CJ} as Functions of MAPP Concentrations.

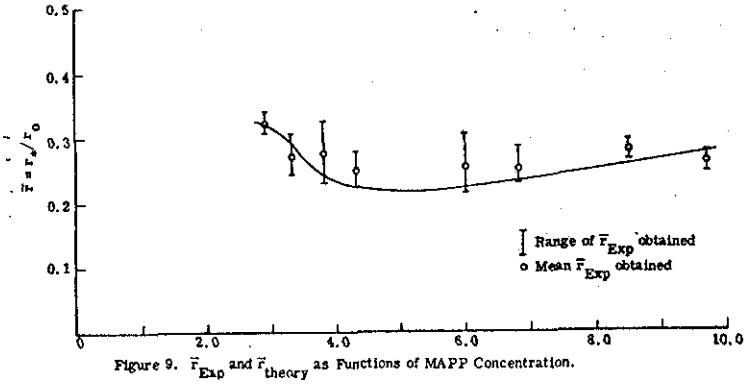

Figure 9. $\bar{r}_{Exp}$ and $\bar{r}_{theory}$ as Functions of MAPP Concentration.

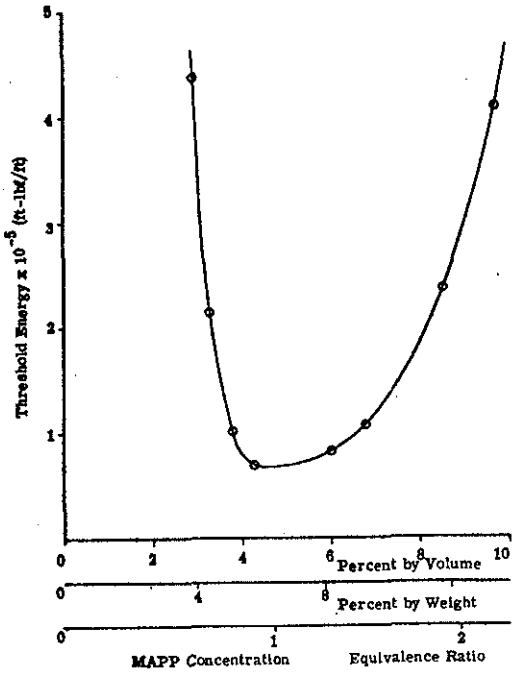

Figure 10. Critical Threshold Energy for Detonation Initiation as a Function of MAPP Concentration in Air.

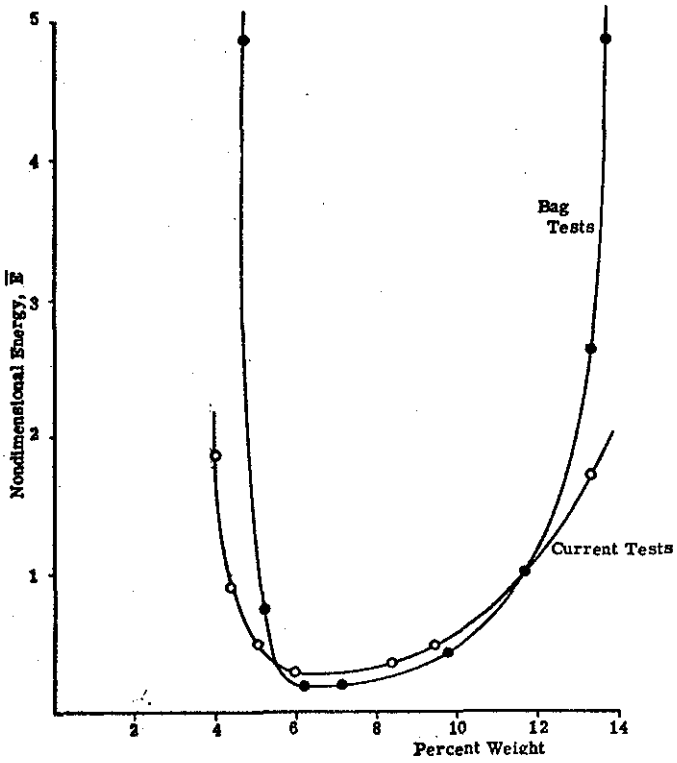

Figure 11. Comparison of Current MAPP-Air Detonation Initiation Limits with "Bag" Test Results.